NANO LETTERS

2008
Vol. 8, No. 4
1212-1218

Close Encounters between Two Nanoshells

J. Britt Lassiter,[†,||] Javier Aizpurua,[⊥] Luis I. Hernandez,[||] Daniel W. Brandl,[†,||] Isabel Romero,[⊥] Surbhi Lal,[‡,||] Jason H. Hafner,[†,§,||] Peter Nordlander,[†,‡,||] and Naomi J. Halas*[,‡,§,||]

Department of Physics and Astronomy, Department of Electrical and Computer Engineering, Department of Chemistry, Laboratory for Nanophotonics, Rice University, Houston, Texas 77005, Donostia International Physics Center and Centro de Fisica de Materiales CSIC-UPV/EHU, Paseo Manuel Lardizabal 4, 20018 San Sebastian, Spain

Received January 28, 2008; Revised Manuscript Received February 28, 2008

ABSTRACT

Plasmonic nanoparticle pairs known as "dimers" embody a simple system for generating intense nanoscale fields for surface enhanced spectroscopies and for developing an understanding of coupled plasmons. Individual nanoshell dimers in directly adjacent pairs and touching geometries show dramatically different plasmonic properties. At close distances, hybridized plasmon modes appear whose energies depend extremely sensitively on the presence of a small number of molecules in the interparticle junction. When touching, a new plasmon mode arising from charge transfer oscillations emerges. The extreme modification of the overall optical response due to minute changes in very reduced volumes opens up new approaches for ultrasensitive molecular sensing and spectroscopy.

It is now well-known that metallic nanostructures can support resonant oscillations of their conduction band electrons, termed localized surface plasmon resonances (LSPR), when illuminated with light of certain frequencies.[1] Plasmons give rise to large enhancements of the local electromagnetic field at the nanostructure surface, an essential aspect of surface-enhanced spectroscopies.[2–9] The plasmonic properties of a nanostructure depend dramatically on its size and shape, as has been demonstrated in studies of nanorods,[10,11] nanocubes,[12,13] nanostars,[14] nanoshells,[15] and numerous other structures. An understanding of how the plasmonic properties depend on geometry enables the rational design of nanostructures tailored for specific applications such as surface-enhanced spectroscopies,[16–18] where one seeks to maximize the electromagnetic field enhancement over specific frequency ranges, or LSPR sensing, where narrow spectral line widths and a high sensitivity to the dielectric environment are desirable.[13]

Directly adjacent nanoparticle pairs, also known as "dimers", give rise to very large field enhancements in their junctions, which make them highly attractive as SERS substrates, with enhancements approaching single-molecule sensitivities.[3–7] Coupling multiple nanoparticles together in chainlike structures has also been suggested as an approach to nanoscale optical waveguiding and focusing.[19–21] Advances in our understanding of plasmonic nanoparticle interactions will greatly facilitate our abilities to design, develop and optimize such coupled-nanoparticle systems.

Plasmonic dimers of various nanoparticles have been studied experimentally and theoretically,[17,22–31] with the general observation that for incident light polarized along the dimer axis, a red-shift of the longitudinal plasmon resonance occurs with decreasing nanoparticle separation. Plasmon hybridization theory applied to nanoparticle dimers has led to the understanding of dimer plasmon modes as the bonding and antibonding hybridized modes of the characteristic plasmons of the constituent nanoparticles, which remain charge neutral.[32–34] Recent attention has begun to focus on the transition that occurs in a dimer as the interparticle separation is reduced to the onset of conductive overlap and beyond.[25,35,36] When a conduction channel is present between two nanoparticles, new longitudinal plasmon modes involving charge oscillations between the two nanoparticles become possible. In this situation, the total charge on each nanoparticle will oscillate in time. As the particles are merged further, these plasmon modes blue-shift to values determined by the aspect ratio of the composite particle.

In this letter, we examine the plasmon interactions of individual pairs of nanoshells in the adjacent and touching regimes (Figure 1). The characteristic plasmon resonances

* Corresponding author. E-mail: halas@rice.edu.
† Department of Physics and Astronomy, Rice University.
‡ Department of Electrical and Computer Engineering, Rice University.
§ Department of Chemistry, Rice University.
|| Laboratory for Nanophotonics, Rice University.
⊥ Donostia International Physics Center and Centro de Fisica de Materiales CSIC-UPV/EHU.

10.1021/nl080271o CCC: $40.75
Published on Web 03/18/2008

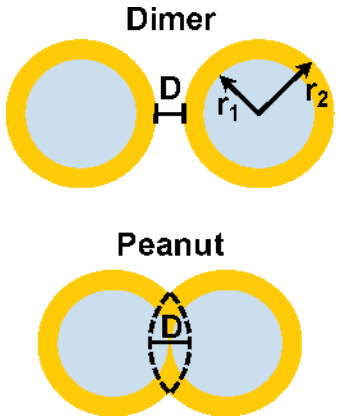

Figure 1. Schematic diagram of the nanoshell dimer and peanut geometries. Individual nanoshells are defined by the core radius r_1 and the overall radius r_2. The distance D is defined as the distance between the outer surfaces of the constituent nanoshells of a peanut or dimer. Thus for dimers, D takes on a positive value and represents the degree of separation, but for peanuts, D takes on a negative value and represents the degree of overlap.

of a nanoshell, already significantly more sensitive to changes in their dielectric environment relative to solid metallic nanoparticles,[37] interact strongly with the plasmon modes of the adjacent nanoshell. Using polarization-dependent dark-field microspectroscopy, we examine the plasmon interaction for weakly and strongly interacting individual proximal nanoshell pairs and for individual touching nanoshell pairs, or "nanopeanuts". Strong polarization dependence for all modes of interaction is observed. With excitation polarization along the dimer axis, for strongly interacting nontouching nanoshell pairs, we observe extremely large LSPR shifts and the excitation of hybridized higher order multipolar plasmon modes. In the touching regime, the plasmon spectrum provides a highly polarization and geometry-dependent signature of a plasmon mode involving electrons flowing back and forth between the two particles. High resolution SEM images reveal important structural details of each dimer and nanopeanut, permitting close comparison of theoretical simulations with experimentally observed plasmonic behavior in all cases.

Nanoshell dimers were fabricated by employing a multi-step process similar to other recently developed dimer fabrication procedures.[38,39] Initially, nanoshells were fabricated as previously reported,[15] then deposited onto a glass coverslip functionalized with 1 wt % poly(vinyl pyridine) (PVP) in ethanol.[40] Next, the nanoshell-coated coverslips were immersed in a 1 mM ethanolic solution of 1-dodecanethiol for 12–24 h, allowing self-assembled monolayers (SAMs) to form onto and passivate the nanoshell surfaces except for the small region of the nanoshell surface that touches the glass slide. The substrate was then removed from solution, rinsed, and sonicated for approximately 4 min in the presence of a 0.1 mM ethanolic solution of 1,9-nonanedithiol. This step removes the nanoshells from the glass surface, exposing the unpassivated surface area of the nanoparticles so that the nonanedithiol molecules can adsorb, linking the nanoshells together to form dimers. Because the majority of the nanoshell surface was passivated before exposure to the linker molecule, the number of nanoshells that can attach to each other is limited, resulting in the preferential formation of dimers rather than extended aggregate structures. The nanostructures were then deposited onto a glass substrate for microspectoscopy measurements. This fabrication procedure results in a mixed dilute ensemble of nanoshell monomers, dimers, some larger n-mers, and fused nanoshell dimers, or nanopeanuts. The nanopeanuts are most likely formed during the initial nanoshell fabrication procedure when two nanoshell precursor nanoparticles adhere to each other before or during the formation of the gold shell. The resulting nanoparticle distribution allows us to directly compare spectra of individual structures on the same substrate and therefore under virtually identical experimental conditions.

To directly compare a specific nanostructure's geometry to its associated spectra, individual structures were first located using environmental scanning electron microscopy (ESEM, FEI Quanta 400) on the glass substrate with respect to a gold finder grid evaporated onto the surface.[41] ESEM allows scanning electron microscopy to be done in a low pressure (here ~2 Torr) water vapor environment so that excess charge can dissipate from the nonconductive substrate. Glass was chosen because it provides an unambiguous substrate for spectroscopy of plasmonic nanostructures that does not strongly modify the plasmon line shape. The orientation angles of both nanoshell dimers and nanopeanuts were measured with respect to the finder grid, such that polarization orientations could be determined during subsequent optical measurements. Our optical setup for unpolarized dark-field microspectroscopy has been presented previously[41,42] but is briefly revisited in the Supporting Information along with a detailed explanation of our setup for polarization dependent microspectroscopy and a discussion of individual nanoshell spectra.

For each structure studied experimentally, exact electrodynamical calculations of the optical response based on the boundary element method (BEM) were performed to examine agreement with experimental results.[43,44] First, the dimensions of each particle along the directions of the measured polarizations were recorded using ESEM. These dimensions served as an initial guide for fitting the experimental data. For dimers, a best fit was obtained by varying the core sizes and the interparticle distance slightly, and for peanuts, the size and separation distance of the cores were varied. The nanoshells were modeled with a core dielectric function for SiO_2[45] and with a shell dielectric function for Au.[46]

Nanoshell dimers show dramatic and easily measurable interparticle plasmon coupling in their polarization-dependent spectra. In Figure 2A, the spectra and corresponding ESEM image of a nanoshell dimer with a relatively large interparticle separation distance on the order of the shell thickness is shown. Here and in the subsequent figures, the black spectrum represents illumination with unpolarized light while the blue (red) spectrum represents illumination that is polarized transverse (longitudinal) with respect to the dimer axis. The longitudinal polarization exhibits only a small red-

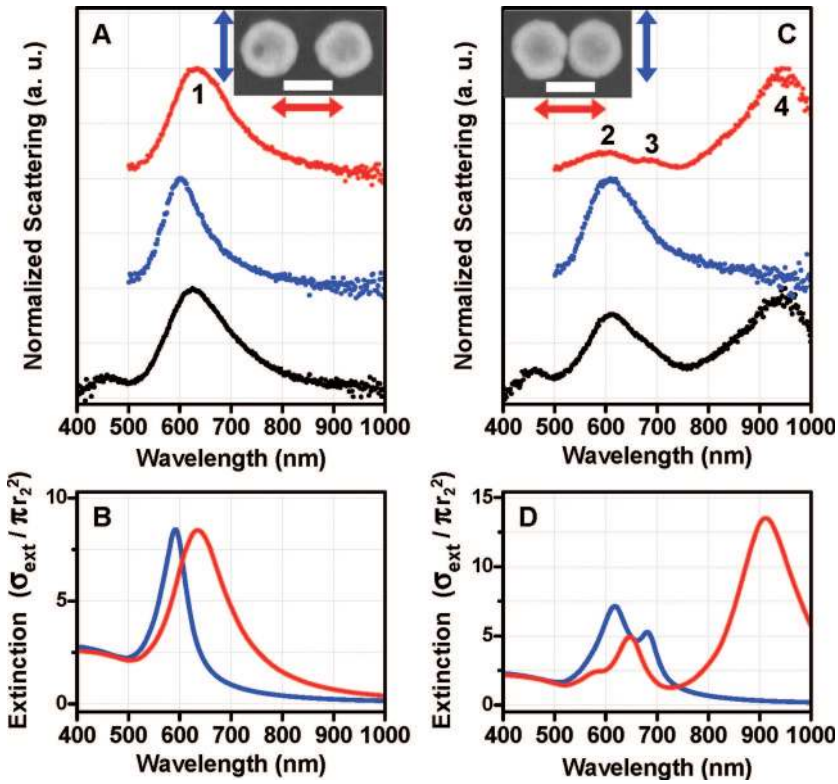

Figure 2. Normalized scattering spectroscopy of nanoshell dimers. Black spectra correspond to unpolarized illumination; blue and red spectra correspond to polarization arrows of the same color in the insets. Inset: ESEM images show the specific dimers for the presented data (scale bar = 100 nm). Peak numbers correspond to numbered energy levels in Figure 3. (A) Experimental data for a weakly interacting dimer. (B) BEM simulations fitting data in (A). Both shells were fit as (r_1, r_2) = (42, 59) nm with D = 20 nm. (C) Experimental data for a strongly interacting dimer. (D) BEM simulations fitting data in (C). Both shells were fit to be slightly elliptical, elongated in the transverse direction: the leftmost shell has a core with semiaxes 45 and 47 nm and an outer shell with semiaxes 58 and 60 nm, while the rightmost shell has a core with semiaxes 42 and 48 nm and an outer shell with semiaxes 55 and 61 nm with D = 1 nm. Simulations are normalized to the physical cross section of a nanoshell.

shift of the dipole plasmon (peak 1), characteristic of a weakly interacting dimer. The simulations reproduce the experimentally obtained spectra quite well (Figure 2B). The small red-shift of the longitudinal dipole plasmon observed experimentally is reproduced qualitatively in the simulations by modeling a dimer with a 20 nm separation distance, a relatively large distance consistent with the ESEM image in Figure 2A. In the weak coupling regime, the shift of the dimer plasmon is small and insensitive to interparticle distance.

For a nanoshell dimer with a much smaller separation distance, the interaction is significantly stronger, exhibiting a much larger red-shift (Figure 2C). Here the ESEM image shows a nanoshell dimer with an interparticle spacing $D \sim$ 1–1.5 nm, consistent with the nanoshells being chemically linked by the nonanedithiol tether molecules.[47] For this dimer, the longitudinal dipolar plasmon mode has red-shifted quite dramatically, to 930 nm. The drastic increase in the degree of red-shifting in this case has two origins. One contribution results from the fact that the interaction is mediated by the electromagnetic near field, which increases rapidly toward the shell surface.[48] The second effect contributing to the magnitude of the plasmon shift is the presence of the linker molecules between the nanoshells of the dimer structure. In our simulations, to achieve quantitative agreement with the experiment required the introduction of a 1 nm thick dielectric layer with a refractive index of 1.42 (corresponding to the SAM) surrounding both shells and the interparticle junction. This effect, which has important implications for nanoparticle-based sensing, will be discussed further below.

Two higher energy modes are also clearly observable in the longitudinally polarized spectrum of the strongly interacting dimer, denoted peaks 2 and 3 (Figure 2C). These features cannot be resolved in the unpolarized spectrum because the longitudinal quadrupolar and octupolar dimer plasmons overlap the transverse dipolar dimer plasmon. The calculated longitudinal polarization spectrum contains three peaks, in good agreement with the experimental observations. However, the transverse polarization spectrum has a double peak structure, which was not experimentally observed. The single mode observed in the transverse polarization for the weakly interacting dimer (Figure 2A) is narrower than the transverse mode in the strongly interacting case (Figure 2C). Therefore, it is possible that the double peak structure is also present in the experimental data but cannot be resolved.

Both the plasmon red-shift associated with the dimers and the observance of higher order modes can be understood in terms of the plasmon hybridization model.[32–34] Schematic diagrams for the plasmon hybridization of nanoshell dimers for these two regimes are shown (Figure 3). While nanoshells themselves are hybridized structures,[32,49] this diagram shows how the bonding dipole modes of each nanoshell hybridize

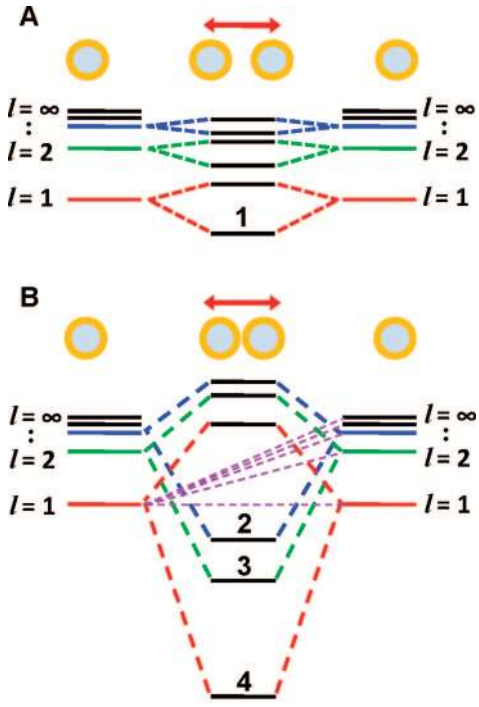

Figure 3. Energy level diagram for plasmon hybridization of nanoshell dimers, in the longitudinal polarization configuration. Numbered energy levels correspond to numbered peaks in Figure 2. (A) Weakly interacting dimer. (B) Strongly interacting dimer.

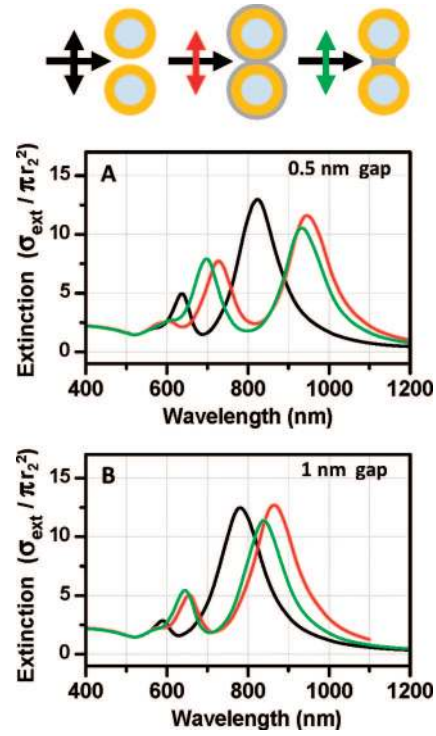

Figure 4. BEM calculations comparing the LSPR shift for nanoshell (longitudinal polarization) for three cases of dielectric surroundings: in vacuum (black), with a dielectric medium both in the interparticle junction and surrounding the outside of the nanoshells (red), and with the dielectric medium only inside the interparticle junction (green). Simulations use the nanoparticle sizes for the dimer in Figure 2C but with a slightly flatter gap size *D* of (A) 0.5 nm and (B) 1 nm.

into longitudinal dimer modes. The effective hybridization of two levels is determined by the ratio of the square of their interaction energy and their energy difference. The weakly interacting dimer case, where the two nanoshells are separated by a relatively large distance, is shown in Figure 3A. The interaction between the two nanoshells results in only a small splitting of the nanoshell modes into bonding and antibonding levels, which essentially retain the same multipolar index, l, as the nanoshell modes from which they originate. In this regime, only the lowest order dipolar $l = 1$ dimer mode (mode 1) is excitable by light because only this mode has a strong dipole moment. As the interparticle distance is decreased and the interparticle coupling increases, the splitting into bonding and antibonding modes becomes much larger than for the weak interaction case (Figure 3B). Also, because of the lack of spherical symmetry of the dimer geometry, the normal modes associated with each individual nanoshell are no longer normal modes in the reference frame of the other nanoshell. Thus in spite of the difference in energy between nanoshell plasmons of different multipolar l, the increased interaction results in the mixing (hybridization) of different multipolar order plasmons such that each dimer mode contains an admixture of different l nanoshell modes (illustrated by the dashed purple lines in Figure 3B).[33,34] This increased coupling has two consequences. First, the lowest order plasmon mode (4) red-shifts much more strongly than a dipole-only interaction would allow because it is, in a sense, repelled by all of the modes with which it interacts. Also, higher order dimer modes can now be excited by light due to the mixing of higher order modes with the dipolar modes of each nanoshell. These higher order features correspond to peaks 2 and 3 in the longitudinal spectrum of Figure 2C.

In nanoshell dimers, the dielectric screening introduced by the molecular linker in the junction between the nanoparticles is remarkably large. In our simulations, we can examine the relative contribution of this molecular layer to the bare coupled-nanoparticle case (Figure 4). Here the strongly interacting nanoshell dimer case is shown for two interparticle distances of 0.5 and 1.0 nm, respectively. For each case, the dimer plasmon spectra are modeled with and without the dielectric spacer layer. Here we can see quite clearly that the dielectric layer results in a very large red-shift compared to the bare dimer case, an effect that increases with decreasing interparticle distance. In our simulations, we also examine the extent to which local changes in the dielectric function in *just the junction region* contribute to this additional dielectric red-shift. This corresponds to "loading" the interparticle junction with molecules, as in surface-enhanced spectroscopy applications. The calculation is performed by adding a finite dielectric volume confined to the junction and comparing this to the case of a complete dielectric coating for the dimer. For an accurate comparison of spectral shifts due to molecular screening, the geometry of the gap is kept exactly equal in the three cases, therefore shifts due to conformational differences can be completely discarded. Figure 4 shows that by far most of the red-shift (90%) is due to the dielectric screening mediated by the

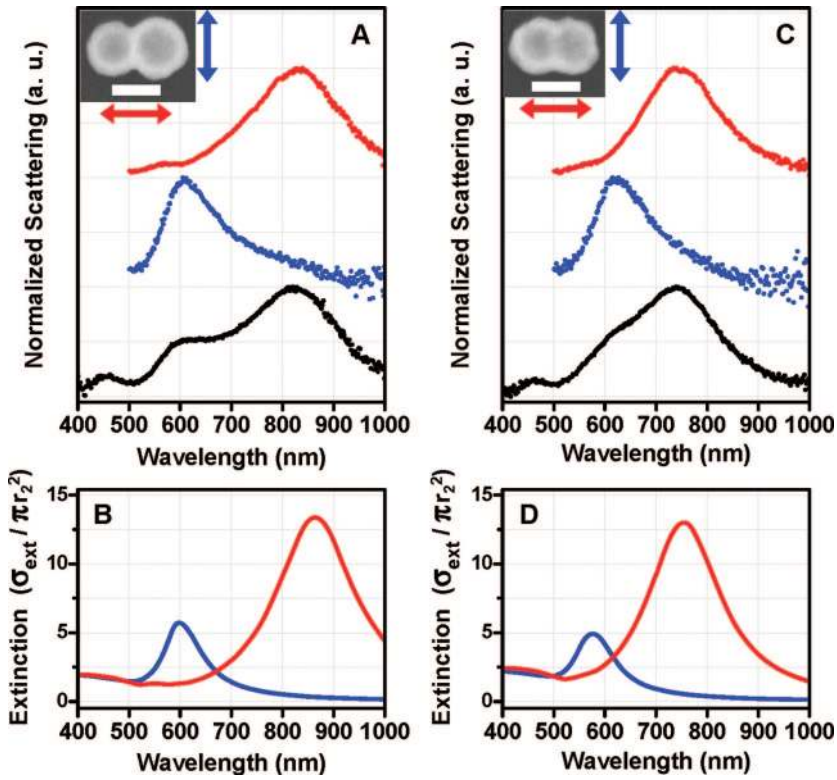

Figure 5. Normalized scattering spectroscopy of nanoshell peanuts. Black spectra correspond to unpolarized illumination; blue and red spectra correspond to polarization arrows of the same colors in the insets. Inset: ESEM images show the specific peanuts for the presented data (scale bar = 100 nm). (A) Experimental data for a peanut with a relatively large separation distance between the two cores. (B) BEM simulations fitting data in (A). This peanut was fitted where the leftmost shell is (r_1, r_2) = (44, 58) nm and the rightmost shell is (r_1, r_2) = (51, 65) nm and D = –20 nm, corresponding to a core separation of 8 nm. (C) Experimental data for a peanut where the cores are almost touching. (D) BEM simulations fitting data in (C). This peanut was fitted where both shells are (r_1, r_2) = (42, 58) nm. D = –30 nm, corresponding to a core separation of only 2 nm. Simulations are normalized to the physical cross section of a nanoshell.

molecules within the interparticle junction, with the molecules exterior to this region barely contributing to the shift. This observation has extremely important implications for the design of junction-based SERS or SEIRA sensors.[18] For SERS, the plasmon line width must span the frequencies of the Raman excitation laser and the excitable Stokes modes of the molecules; for SEIRA, the plasmon frequencies must correspond directly to the dipole-active vibrational modes of the adsorbate molecule. Such large plasmon shifts that occur in this geometry must be accounted for when designing a nanosensor substrate, or the presence of the analyte molecules themselves will "detune" the plasmon resonance from the source. This highly sensitive effect may also be exploitable in the design of SPR sensors based on plasmonic junctions for single- or few-molecule detection.

The nanopeanut geometry allows us to experimentally investigate nanoshell dimers in the unusual "merged" regime, in comparison with the nontouching dimer regime. Two cases of nanopeanuts, differing in degree of overlap, were examined (Figure 5). For each case, the unpolarized spectrum contains two major peaks, which resolve into one red-shifted longitudinal mode and a transverse mode located at shorter wavelengths. The two examples differ, however, in the size of the red-shift of the longitudinal plasmon. When the overlap between the two nanoshells is small enough that a significant layer of gold separates the two cores from touching each other (Figure 5A), the longitudinal plasmon remains strongly red-shifted with respect to a monomer. Here, this mode was positioned at 820 nm, corresponding to a core separation of 8 nm ($D = -20$ nm) as fit using BEM calculations (Figure 5B). We note that for this nanopeanut, the two constituent nanoshells do differ in size, but the degree of overlap plays a more significant role in determining the spectrum. For significant conducting overlap, the plasmon energies are determined primarily by the aspect ratio of the composite particle.[35] In our second example (Figure 5C), the ESEM image indicated that little or no gold separated the two cores. The longitudinal mode at 740 nm is therefore blue-shifted in comparison to the previous case. The calculations fit the data very well in both cases, reproducing the positions of the longitudinal mode as well as the transverse mode, which lends confidence to the accuracy of the obtained D values. Despite the fact that one can generally distinguish a core and a shell in the contrast of the ESEM images, the precise separation distance between the cores inside a peanut cannot be determined from the images. It is interesting to note that, in this case, fitting the plasmon spectra with simulations provides the best route to determine this information. These two cases are consistent with our picture of the merged regime, where the longitudinal plasmon blue-shifts as the overlap of a nanopeanut increases, in agreement with previous theoretical[35] and experimental[25] findings for solid merged nanoparticles.

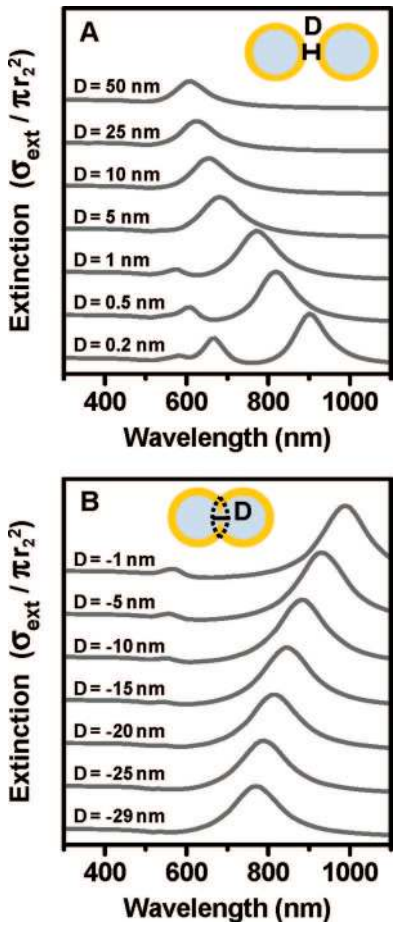

Figure 6. Boundary element method simulations for nanoshell dimers (A) and nanoshell peanuts (B). The constituent nanoshells have (r_1, r_2) = (40, 55) nm. The distances D between the constituent nanoshells are listed for each spectrum. For dimers, D represents the separation distance between the two nanoshell surfaces. For peanuts, D represents the amount of overlap of the metal shells and is therefore negative. Extinction cross sections are normalized to the physical cross section of a single nanoshell.

In Figure 6, we show the evolution of the longitudinal plasmon frequencies of two nanoshells as their separation D is reduced from positive to negative (overlapping) values. For nontouching dimers, the dipole peak red-shifts and higher order modes begin to appear for the short separations. When the two shells cross over into the merged regime (negative D), the longitudinal mode starts to blue-shift. The trends of both the nanoshell dimer and the peanut are consistent with the previous studies concerning solid metal nanoparticles.[25,35]

In conclusion, using polarization-dependent single nanostructure spectroscopy we have investigated the plasmon resonances of two nearby nanoshells as their separation is reduced from the nontouching to the touching regimes. The position and shape of the scattering spectra are found to be dramatically different in these regimes. In the nontouching regime, dimer plasmons are formed through hybridization of the individual multipolar nanoshell plasmons with each nanoparticle remaining neutral. For large separations, the spectra exhibit a single polarization-dependent resonance that can be identified as a bonding dimer resonance formed from the hybridization of the dipolar resonances of each nanoshell. For two nontouching nanoshells placed at close proximity to each other, the spectra exhibit several higher multipolar dimer resonances that become dipole-active through the mixing with the dipolar plasmon resonances of the individual nanoshells. In this regime, the dimer plasmons exhibit a remarkable sensitivity to the presence of dielectric media in the junction. When the nanoshells are touching, the spectra exhibit a single plasmon resonance which involves electrons flowing between the two particles. This charge transfer plasmon is found to blue-shift as the nanoshells move closer together. The large variations in optical response due to slight conformational and environmental changes revealed in this study will transform this canonical structure into a very versatile system for plasmonic sensing and spectroscopy.

Acknowledgment. The Rice group acknowledges financial support from the U.S. Army Research Laboratory and Army Research Office under grant W911NF-04-1-0203, the Robert A. Welch Foundation under grants C-1220 (P.N.) and C-1222 (N.J.H.) and by NSF under grant EEC-0304097 and the IGERT Fellowship of J.B.L. under DG-0504425. J.A. acknowledges the hospitable and friendly atmosphere at the Lab for Nanophotonics in Houston during his one month stay in summer 2007, where most of this work was developed.

Supporting Information Available: Experimental procedures. Schematic diagram for polarization dependent dark-field microspectroscopy. Normalized scattering spectroscopy of a single nanoshell. This material is available free of charge via the Internet at http://pubs.acs.org.

References

(1) Kelly, K. L.; Coronado, E.; Zhao, L. L.; Schatz, G. *J. Phys. Chem. B* **2003**, *107*, 668.
(2) Moskovits, M. *Rev. Mod. Phys.* **1985**, *57*, 783.
(3) Nie, S.; Emory, S. R. *Science* **1997**, *275*, 1102.
(4) Kneipp, K.; Wang, Y.; Kneipp, H.; Perelman, L. T.; Itzkan, I.; Dasari, R. R.; Feld, M. S. *Phys. Rev. Lett.* **1997**, *78*, 1667.
(5) Xu, H.; Bjerneld, E. J.; Käll, M.; Börjesson, L. *Phys. Rev. Lett.* **1999**, *83*, 4657.
(6) Michaels, A. M.; Nirmal, M.; Brus, L. E. *J. Am. Chem. Soc.* **1999**, *121*, 9932.
(7) Michaels, A. M.; Jiang, J.; Brus, L. *J. Phys. Chem. B* **2000**, *104*, 11965.
(8) Xu, H.; Aizpurua, J.; Käll, M.; Apell, P. *Phys. Rev. E* **2000**, *62*, 4318.
(9) Osawa, M. *Top. Appl. Phys.* **2001**, *81*, 163.
(10) Link, S.; El-Sayed, M. A. *J. Phys. Chem. B* **1999**, *103*, 8410.
(11) Murphy, C. J.; Sau, T. K.; Gole, A.; Orendorff, C. J. *MRS Bull.* **2005**, *30*, 349.
(12) Sun, Y.; Xia, Y. *Science* **2002**, *298*, 2176.
(13) Sherry, L. J.; Chang, S.-H.; Schatz, G. C.; Duyne, R. P. V.; Wiley, B. J.; Xia, Y. *Nano Lett.* **2005**, *5*, 2034.
(14) Nehl, C. L.; Liao, H.; Hafner, J. H. *Nano Lett.* **2006**, *6*, 683.
(15) Oldenburg, S. J.; Averitt, R. D.; Westcott, S. L.; Halas, N. J. *Chem. Phys. Lett.* **1998**, *288*, 243.
(16) Jackson, J. B.; Halas, N. J. *Proc. Natl. Acad. Sci. U.S.A.* **2004**, *101*, 17930.
(17) Talley, C. E.; Jackson, J. B.; Oubre, C.; Grady, N. K.; Hollars, C. W.; Lane, S. M.; Huser, T. R.; Nordlander, P.; Halas, N. J. *Nano Lett.* **2005**, *5*, 1569.
(18) Wang, H.; Kundu, J.; Halas, N. J. *Angew. Chem., Int. Ed.* **2007**, *46*, 9040.
(19) Maier, S. A.; Brongersma, M. L.; Kik, P. G.; Meltzer, S.; Requicha, A. A. G.; Atwater, H. A. *Adv. Mater.* **2001**, *13*, 1501.
(20) Maier, S. A.; Kik, P. G.; Atwater, H. A.; Meltzer, S.; Harel, E.; Koel, B. E.; Requicha, A. A. G. *Nat. Mater.* **2003**, *2*, 229.
(21) Li, K.; Stockman, M. I.; Bergman, D. J. *Phys. Rev. Lett.* **2003**, *91*, 227402.

(22) Tamaru, H.; Kuwata, H.; Miyazaki, H. T.; Miyano, K *Appl. Phys. Lett.* **2002**, *80*, 1826.
(23) Rechberger, W.; Hohenau, A.; Leitner, A.; Krenn, J. R.; Lamprecht, B.; Aussenegg, F. R. *Opt. Commun.* **2003**, *220*, 137.
(24) Prikulis, J.; Svedberg, F.; Käll, M.; Enger, J.; Ramser, K.; Goksör, M.; Hanstorp, D. *Nano Lett.* **2004**, *4*, 115.
(25) Atay, T.; Song, J.-H.; Nurmikko, A. V. *Nano Lett.* **2004**, *4*, 1627.
(26) Gunnarsson, L.; Rindzevicius, T.; Prikulis, J.; Kasemo, B.; Käll, M.; Zou, S.; Schatz, G. C. *J. Phys. Chem. B* **2005**, *109*, 1079.
(27) Sönnichsen, C.; Reinhard, B. M.; Liphardt, J.; Alivisatos, A. P. *Nat. Biotechnol.* **2005**, *23*, 741.
(28) Reinhard, B. M.; Siu, M.; Agarwal, H.; Alivisatos, A. P.; Liphardt, J. *Nano Lett.* **2005**, *5*, 2246.
(29) Wang, H.; Halas, N. J. *Nano Lett.* **2006**, *6*, 2945.
(30) Ringler, M.; Klar, T. A.; Schwemer, A.; Susha, A. S.; Stehr, J.; Raschke, G.; Funk, S.; Borowski, M.; Nichtl, A.; Kürzinger, K.; Phillips, R. T.; Feldman, J. *Nano Lett.* **2007**, *7*, 2753.
(31) Jain, P. K.; Huang, W.; El-Sayed, M. A. *Nano Lett* **2007**, *7*, 2080.
(32) Prodan, E.; Radloff, C.; Halas, N. J.; Nordlander, P. *Science* **2003**, *302*, 419.
(33) Nordlander, P.; Oubre, C.; Prodan, E.; Li, K.; Stockman, M. I. *Nano Lett.* **2004**, *4*, 899.
(34) Brandl, D. W.; Oubre, C.; Nordlander, P. *J. Chem. Phys.* **2005**, *123*, 024701.
(35) Romero, I.; Aizpurua, J.; Bryant, G. W.; Abajo, F. J. G. d. *Opt. Express* **2006**, *14*, 9988.
(36) Danckwerts, M.; Novotny, L. *Phys. Rev. Lett.* **2007**, *98*, 026104.
(37) Sun, Y.; Xia, Y. *Anal. Chem.* **2002**, *74*, 5297.
(38) Zhao, J.; Haes, A. J.; Zhang, X.; Zou, S.; Hicks, E. M.; Schatz, G. C.; Duyne, R. P. V. *Mater. Res. Soc. Symp. Proc.* **2006**, *900E*, 0900-O13-08.1-0900-O13-08.6.
(39) Sardar, R.; Heap, T. B.; Shumaker-Parry, J. S. *J. Am. Chem. Soc.* **2007**, *129*, 5356.
(40) Malynych, S.; Luzinov, I.; Chumanov, G. *J. Phys. Chem. B* **2002**, *106*, 1280.
(41) Nehl, C. L.; Grady, N. K.; Goodrich, G. P.; Tam, F.; Halas, N. J.; Hafner, J. H. *Nano Lett.* **2004**, *4*, 2355.
(42) Wang, H.; Wu, Y.; Lassiter, B.; Nehl, C. L.; Hafner, J. H.; Nordlander, P.; Halas, N. J. *Proc. Natl. Acad. Sci. U.S.A.* **2006**, *103*, 10856.
(43) Garcia de Abajo, F. J.; Howie, A. *Phys. Rev. Lett.* **1998**, *80*, 5180–5183.
(44) Garcia de Abajo, F. J.; Howie, A. *Phys. Rev. B* **2002**, *65*, 115418.
(45) Palik, E. D. *Handbook of Optical Constants of Solids*; Academic Press: New York, 1985.
(46) Johnson, P. B.; Christy, R. W. *Phys. Rev. B* **1972**, *6*, 4370.
(47) Porter, M. D.; Bright, T. B.; Allara, D. L.; Chidsey, C. E. D. *J. Am. Chem. Soc.* **1987**, *109*, 3559.
(48) Lal, S.; Grady, N. K.; Goodrich, G. P.; Halas, N. J. *Nano Lett.* **2006**, *6*, 2338.
(49) Prodan, E.; Nordlander, P. *J. Chem. Phys.* **2004**, *120*, 5444.

NL080271O